

Scale-up of a Cold Flow Model of FICFB Biomass Gasification Process to an Industrial Pilot Plant – Hydrodynamics of Particles

J. MELE, J. OMAN, J. KROPE*

University of Ljubljana

Faculty of Mechanical Engineering

Aškerčeva 6, 1000 Ljubljana, SLOVENIA

University of Maribor, Faculty of chemistry and chemical engineering

Smetanova 17, 2000 Maribor, SLOVENIA

jernej.mele@bosio.si, janez.oman@fs.uni-lj.si, juri.krope@uni-mb.si

Abstract: - The article introduces the research of particles hydrodynamics in a cold flow model of FICFB biomass gasification process and its scale-up to industrial pilot plant. A laboratory unit has been made for the purposes of experimental research. The laboratory unit is three times smaller than the later pilot plant. For a reliable observation of the flow process, similar flow conditions must be created in the laboratory unit and the pilot plant. The results of the laboratory model will be similar to those of the actual device if geometry, flow and Reynolds numbers are the same. Therefore, there is no need to bring a full-scale gasificator into the laboratory and actually test it. This is an example of "dynamic similarity".

Key words: - Fluid bed, Pneumatic transport, Reynolds number, Gasification, Scale-up

1 Introduction

Fast Internal Circulating Fluid Bed (FICFB) biomass gasification is a process for producing high caloric synthesis gas (syngas) from solid Hydrocarbons. The basic idea is to separate syngas from flue gas, and due to the separation we have a gasification zone for endothermic reactions and a combustion zone for exothermic reactions. The bed material circulates between these two zones and serves as a heat carrier and a catalyst.

While researching the 250kW FICFB pilot plant certain questions concerning particle dynamics in gas flows appeared. There is a zone where fluid bed conditions are made with superheated steam, pneumatic transport with hot air and a pair of secondary gas inlets. These particle flows are difficult to describe with mathematical models. This is the main reason why the three-times smaller cold-flow laboratory unit has been made. The hydrodynamics of particles will be studied in the air flow. Flows in the laboratory unit and pilot plant must be similar for a reliable evaluation of the process in the pilot plant.

2 Laboratory unit

The laboratory unit is a device three times smaller than the pilot plant. Its main purpose is to simulate the hydrodynamic process of FICFB gasification in a cold flow. It is made from stainless steel and in the case of the parts that are of greatest interest to the present study is made of glass, so that the particle behaviour may be observed. Fig. 1 shows a model of laboratory unit. Its main elements are:

- Reactor (A),
- Cyclone (C),
- Siphon (D),
- Combustion zone (B),
- Gas distributor (J_1 and J_2),
- Auxiliary inlets (I_1 and I_2).

Trough experiments on the laboratory unit the effectiveness of elements will be studied so as to enable the correction and improvement of any construction flaws they contain. Fig. 2 shows the laboratory unit that will be used for studying the flow process. There are 7 places for pressure, 2 for temperature and 2 for gas flow measurements. For the proper operation of our solid flow system it is vital that the particles are maintained in dynamic suspension as settling down the particles can clog both the measuring openings and injection nozzles. Thus it is essential to design such systems with special care. All measurements involving the risk of clogging the measuring opening must be taken outside the solid flow cone if possible – gas flow velocity measurements with the Pitot tube must be taken in the gas pipeline before gas enters the gasificator. It is highly desirable for all measuring openings to be small and positioned at right angles to the direction of flow.

Table 1: Main dimensions of laboratory unit and pilot plant

	Laboratory unit	Pilot plant
$D_{\text{gas},1}$ [mm]	100	300
$D_{\text{gas},2}$ [mm]	190	600
D_{comb} [mm]	50	150
h_{comb} [mm]	1500	4500

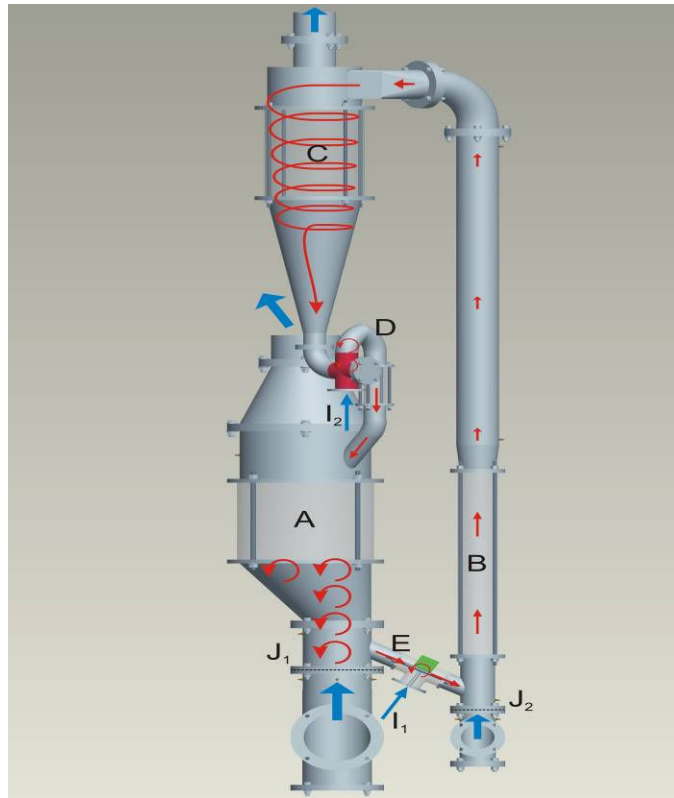


Fig. 1: 3D model of laboratory unit



Fig. 2: Laboratory unit

3 Basic equations for describing the fluidized state and similarity of flows

3.1 Reynolds number

The goal herein is to compare flows in the laboratory unit to those in the pilot plant. In order for the two flows to be similar they must have the same geometry and equal Reynolds numbers. When comparing fluid behaviour at homologous points in a model and a full-scale flow, the following holds:

$Re(\text{laboratory unit}) = Re(\text{Scale-up pilot plant})$

The Reynolds number of particles can be determined by the following equation [1, 2]:

$$Re_p = \frac{D_p \cdot v_g \cdot \rho_g}{\eta_g} \quad (1)$$

For achieving the required similarity, the following conditions must be also fulfilled:

$$\frac{p}{\rho_g \cdot v_g^2} = \frac{p_{g,ar}}{\rho_{g,ar} v_{g,ar}^2} \quad (2)$$

3.2 Minimal fluidizing velocity

The fluidization state starts when the drag force of by upward moving gas equals the weight of the particles

$$F_{g-p} = \frac{1}{2} \cdot C_x \cdot A_p \cdot \rho_p \cdot v_g^2 \quad (3)$$

or

$$\Delta p \cdot A_t = (A_t \cdot L_{mf})(1 - \varepsilon_{mf}) \left[(\rho_s - \rho_g) \frac{g}{g_c} \right] \quad (4)$$

By rearranging equation (4), for minimum fluidizing conditions we find the following expression [1],

$$\frac{\Delta p_{mf}}{L_{mf}} = (1 - \varepsilon_{mf}) (\rho_s - \rho_g) \frac{g}{g_c} \quad (5)$$

Voidage in fluidized bed ε_{mf} is larger than in the packed bed and it can be estimated experimentally from a random ladling sample. For small particles and low Reynolds numbers the viscous energy losses predominate and the equation simplifies to [1]:

$$v_{mf} = \frac{(\Phi_s \cdot D_p)^2}{150} \cdot \frac{\rho_p - \rho_g}{\eta_g} \cdot g \cdot \frac{\varepsilon_{mf}^2}{(1 - \varepsilon_{mf})} \quad (6)$$

for $Re_p < 20$

For large particles only the kinetic energy losses need to be considered:

$$v_{mf} = \sqrt{\frac{\Phi_s \cdot D_p}{1,75} \cdot \frac{(\rho_p - \rho_g)}{\eta_g} \cdot g \cdot \varepsilon_{mf}^3} \quad (7)$$

for $Re_p > 1000$.

If Φ_s and ε_{mf} are unknown, the following modifications suggested by *Wen and Yu* [1] are used:

$$\frac{1 - \varepsilon_{mf}}{\Phi_s^2 \cdot \varepsilon_{mf}^2} \cong 11 \quad (8)$$

$$\frac{1}{\Phi_s \cdot \varepsilon_{mf}^3} \cong 14 \quad (9)$$

Equations (5) and (6) can now be simplified to:

$$v_{mf} = \frac{D_p^2 \cdot (\rho_p - \rho_g) \cdot g}{1650 \cdot \eta_g} \quad (10)$$

for $Re_p < 20$

$$v_{mf} = \sqrt{\frac{D_p \cdot g \cdot (\rho_p - \rho_g)}{24,5 \cdot \rho_g}} \quad (11)$$

for $Re_p > 1000$.

3.3 Terminal velocity

The upper limit of gas flow rate is approximated by the terminal (free fall) velocity of the particles, which can be estimated from the fluid mechanics [1]:

$$v_t = \sqrt{\frac{4 \cdot g \cdot D_p \cdot (\rho_p - \rho_g)}{3 \cdot \rho_g \cdot C_x}} \quad (12)$$

There are spherical and non-spherical particle shapes in the bed and each of them has a different C_x

value. If we combine equations (1) and (12) we get the velocity independent group:

$$C_x Re_p^2 = \frac{4 \cdot g \cdot D_p^3 \cdot \rho_g \cdot (\rho_p - \rho_g)}{3 \cdot \eta_g^2} \quad (13)$$

An alternative way of finding v_t for spherical particles uses analytical expressions for the drag coefficient C_x [1].

$$C_x = \frac{24}{Re_p} \quad \text{for} \quad Re_p < 0,4 \quad (14)$$

$$C_x = \frac{10}{\sqrt{Re_p}} \quad \text{for} \quad 0,4 < Re_p < 500 \quad (15)$$

$$C_x = 0,43 \quad \text{for} \quad 500 < Re_p < 200000 \quad (16)$$

But still no simple expression can represent the experimental findings for the entire range of Reynolds numbers, so by replacing these values C_x in equation (12) we obtain:

$$v_t = \frac{(\rho_p - \rho_g) \cdot g \cdot D_p^2}{18 \cdot \eta_g} \quad (17)$$

for $Re_p < 0,4$

$$v_t = \sqrt[3]{\frac{4 \cdot (\rho_p - \rho_g)^2 \cdot g^2}{225 \cdot \eta_g \cdot \rho_g}} \cdot D_p \quad (18)$$

for $0,4 < Re_p < 500$

and

$$v_t = \sqrt{\frac{3,1 \cdot D_p \cdot g \cdot (\rho_p - \rho_g)}{\rho_g}} \quad (19)$$

for $500 < Re_p < 200000$.

3.4 Determining density and dynamical viscosity of gas mixtures

In the pilot plant we will have multiple gas mixtures at different temperatures due to chemical reactions. For our calculations the density and dynamical viscosity for these mixtures will be determined by the following equations [7]:

$$\rho_g = \left(\sum_i \frac{w_i}{\rho_i} \right)^{-1} \quad (20)$$

$$\eta_g = \left(\sum_i \frac{w_i}{\eta_i} \right)^{-1} \quad (21)$$

To calculate the density of the gas mixture at an arbitrary temperature and an arbitrary pressure the density under normal condition must be calculated according to equation (20), with the obtained value being converted to density at the required parameters:

$$\rho_{g,ar} = \rho_g \cdot \frac{p_{g,ar}}{p_n} \cdot \frac{T_n}{T_{g,ar}} \quad (22)$$

3.5 Pressure drops

With increased gas velocity of the small solid particles across the bed a characteristic state occurs. Pressure drop starts to increase, reaching its maximum value Δp_{mf} at minimum fluidization velocity v_{mf} . At this point only part of the bed is fluidized. When the bed is fully fluidized (at v_{mff}), the pressure drop is reduced to Δp_{mff} and is almost constant until gas reaches terminal velocity. If the velocity is still increasing, the particles start transporting pneumatically and pressure drop reduces rapidly to 0. By rearranging equation (5), we obtain the following expression [1]:

$$\Delta p_{mf} = (1 - \epsilon_{mf}) (\rho_s - \rho_g) \cdot g \cdot L_{mf} \quad (23)$$

The expression can also be extended to the fully fluidized state [16]:

$$\Delta p_{mff} = (1 - \epsilon_{mff}) (\rho_s - \rho_g) \cdot g \cdot L_{mff} \quad (24)$$

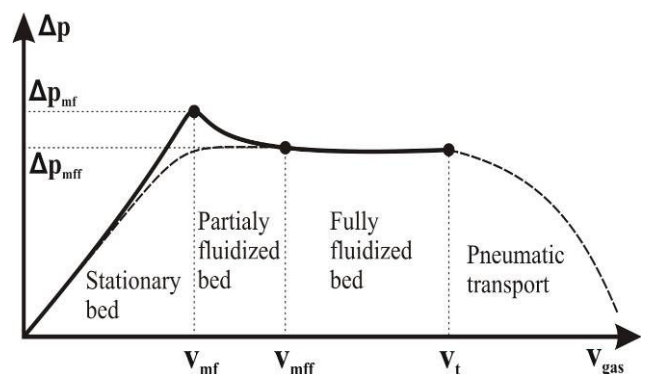


Fig. 3: The change in pressure drop relative to gas velocity

3.6 Mass flows

For a regular flow process we have to ensure proper gas flows at the inlets. Through defining minimal fluidizing and terminal velocities, we can estimate the mass flow of the air reactor and combustion zone by applying the following relations:

$$\phi_{m_g} = \rho_g \cdot v_g \cdot \frac{\pi \cdot D_{tube}^2}{4} \quad (25)$$

$$\phi_{V_g} = \frac{\phi_{m_g}}{\rho_g} \quad (26)$$

4 Calculation analyses

On the basis of the previously-mentioned equations, we can make an estimation of flow conditions in the reactor and combustion zone. We have made a tabular comparison of physical properties between the laboratory unit and pilot plant in tables 2 and 3. The comparison is based on the established equality of Reynolds numbers. As mentioned in chapter 3.1. "In order for two flows to be similar they must have the same geometry and equal Reynolds numbers". In the laboratory unit, flows will be made with upward-blowing air at room temperature whereas in the pilot plant the fluid bed will be made with inlet of superheated steam and pneumatic transport with hot air blowing at 550°C.

Table 2: Physical properties

	Reactor	
	Laboratory unit	Pilot plant
Gas	Air	Steam / Syngas
T [°C]	30	550 / 800
D _p [μm]	200	600
ρ _p [kg/m ³]	8250	3025
ρ _g [kg/m ³]	1,204	0,288 / 0,192
η [Pas]	1,8·10 ⁻⁵	3,1·10 ⁻⁵ / 4,6·10 ⁻⁵
v _{Re<20} [m/s]	0,11	0,21 / 0,14
v _{Re>1000} [m/s]	0,75	1,58 / 1,95
Φ _m [kg/h]	6,4	158,9
Φ _V [m ³ /h]	5,4	548,5
Re _p	9,8	9,0 / 4,9

In the meantime endothermic chemical reactions of pyrolysis, a water-gas-shift reaction will take place in the reactor while exothermic combustion occurs in the combustion zone. Flue gases will have a the temperature of around 1000°C on exiting the combustor and syngas a temperature of approximately 800°C at the reactor's point of exit. Gases in the pilot plant will have lower densities and

higher viscosities than the air in the laboratory unit. The bed material will be Olivine with D_p=600μm. In order to establish similar conditions, we have to use smaller and denser particles. We have chosen brass particles with D_p=200μm. Simulation will also be tested with quartz sand and olivine.

Table 3: Physical properties

	Combustion zone	
	Laboratory unit	Pilot plant
Gas	Air	Air / Flue gas
T _g [°C]	30	550 / 1000
D _p [μm]	200	600
ρ _p [kg/m ³]	8250	3025
ρ _g [kg/m ³]	1,204	0,61/0,294
η [Pas]	1,8·10 ⁻⁵	3,8·10 ⁻⁵ /4,7·10 ⁻⁵
v _{Re<0,4} [m/s]	10,1	15,7/12,6
v _{0,4<Re<500} [m/s]	3,6	5,3/6,2
v _{500<Re<200000} [m/s]	6,6	9,6/13,7
Φ _m [kg/h]	47,7	154,2
Φ _V [m ³ /h]	39,6	524,5
Re _p	46,6	50,8 / 23,3

On the basis of studied flow velocities, mass flows, as well as pressure drops through air distributors and fluid beds at different points of the laboratory unit, we may anticipate the similar results in the pilot plant.

5 Experimental work

5.1 Process description

Firstly, let us look at the process. There are two gas distributors at the bottom of the reactor and combustion zone, through which air is blown vertically. The pneumatic transport of the particles takes place in the combustion zone, where they are separated from the air flow in cyclone and finally gathered in siphon. The second auxiliary inlet acts to fluidize the gathered particles and transport them to the reactor. Here, the fluidized bed is created with the upward blowing air. From here, the particles are transported to the combustion zone through the chute and the speed of transportation is regulated by means of the first auxiliary inlet.

5.2 Openings for pressure measuring

We are primarily interested in how to establish a stationary and self-sustainable process. In the laboratory unit there are glass parts through which the process in course can be directly observed. However, in the hot flow model we will not be able to see what happens inside the pilot plant, and therefore our control system must be able to initiate

the process, keep it in a stationary state and halt it on the basis of measured data such as relative pressure and flow velocities. As previously mentioned, our

laboratory unit consists of 7 pressure and 2 flow velocity measuring points. Fig. 4 details the positions of the pressure places.

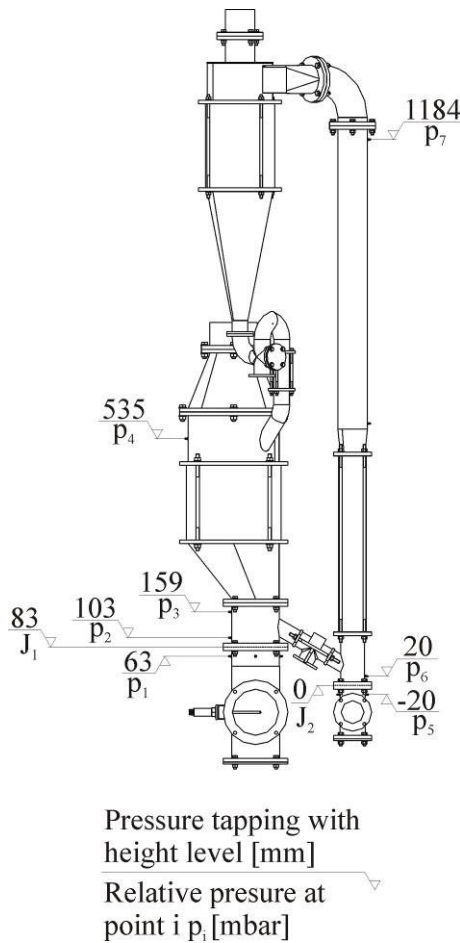


Fig. 4: Openings for the measuring of pressure

Firstly, we have to establish the fluidized bed in the reactor. The particles will fill the chute and the lower part of the combustion zone. The chute is installed at the bottom of the reactor and combustion zone and has an inclination angle. The fluidizing of the particles in the chute will then be started, along with the simultaneous initialization of the pneumatic transport of the particles. When sufficient material has been gathered in the siphon, the particles must be transported back to the reactor with the help of the first auxiliary inlet. The particles are now at their starting point. We must achieve a pressure at the bottom of the fluidized bed p_2 which is larger than that at the point where the chute connects to the combustion zone p_6 . The gas flow direction will be from the reactor to the combustion zone, pushing the particles in the desired direction. At the top of the fluidized bed we have pressure p_4 which has to be lower than p_7 , so the particles can now travel back to the reactor. But there has to be enough material in the siphon at all times in order to prevent the mixing

of gases between the zones. Therefore, the siphon has to serve as seal gap for gases but not for material. The more gas goes through the siphon the lower the caloric value of the gas will be. Experiments will show how pressures are distributed across the system. Fig. 5 shows which measured pressures are of greatest interest for our purposes.

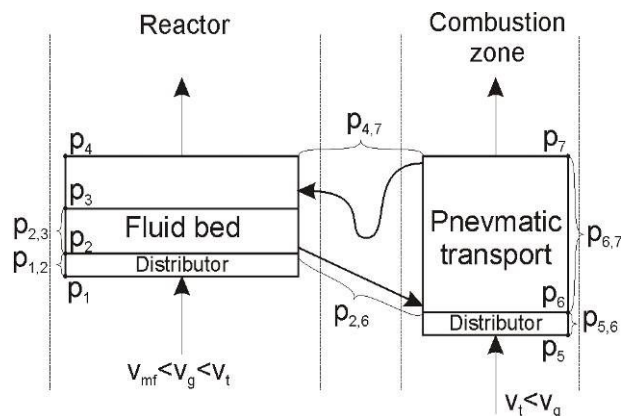


Fig. 5: Measuring scheme

5.3 Distributor

For the distributor 3 metal nets with openings of 225 μ m have been used, with ceramic wool of 8mm placed in between as shown in fig. 6. We tried to achieve a sufficient pressure drop as to attain equal flow through the openings. According to Agarwal recommendation [1, 6], the pressure drop across distributors must be 10% of the pressure drop across the bed, with a minimum of 35 mm H₂O. With this we are in approximate agreement. At higher pressure drops across the distributor we get more particulate or smooth fluidization with less channeling, slugging and fluctuation in density. The pressure drop across the distributor is shown in fig. 7.

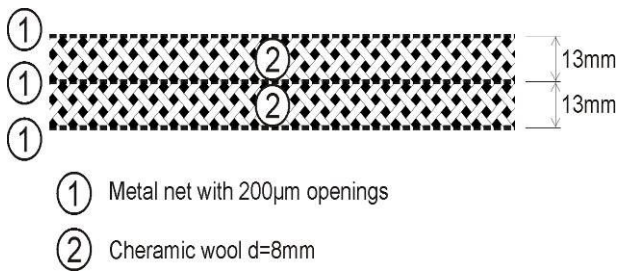


Fig. 6: Distributor structure

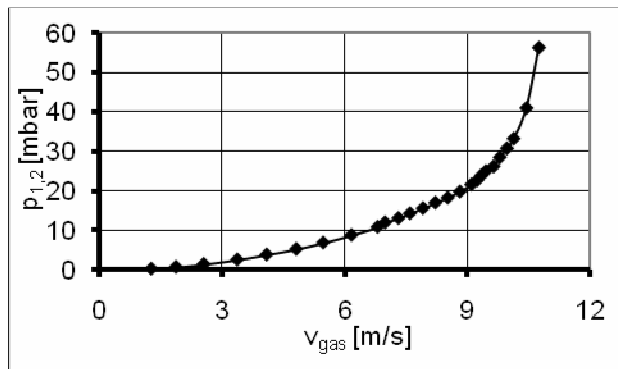


Fig. 7: Pressure drop across the distributor with blowing of air

5.4 Pressure drops across the bed

By way of example, we will look at the experiment with quartz sand. The size of the particles used for simulation is shown in fig. 9. The particles have an average diameter of about 210 μ m. A series of measurements were made and pressure drops at different bed heights taken. Fig. 7 represents a comparison of pressure drop across the bed in the reactor with the gas velocity for different bed heights.

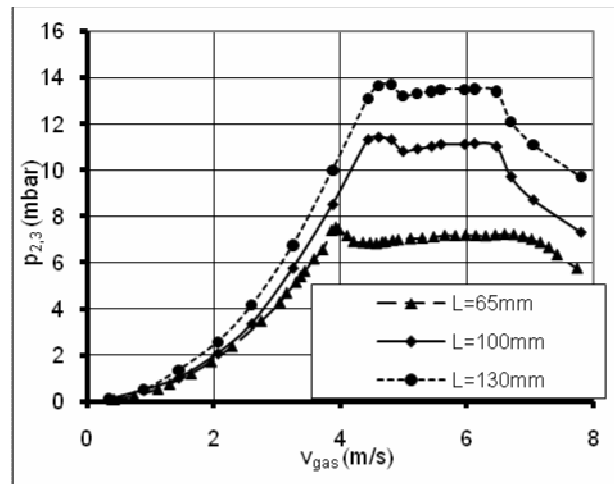


Fig. 8: Pressure drops over fluidized bed

In lower beds less aggregative bubbling occurs and results closer to calculated values are obtained. Nevertheless, still there is a lot of deviation between them. In addition, there is some leakage of gas from the reactor through chute to the combustion zone and as the Pitot tubes are placed in front of gas entering each zone those velocities do not represent the real situation, although the mass flow of air blown through unit is quite as predicted. Comparisons of error between calculations and experimental results are presented in fig. 9 and 10. However, gas velocity is almost impossible to measure within the laboratory unit because attempts to do so would inevitably lead to bed material clogging the measure openings in the device. Having said that, our assessment and purpose is to define and achieve a stationary process on the basis of the measuring system. The measured quantities are presented in table 3.

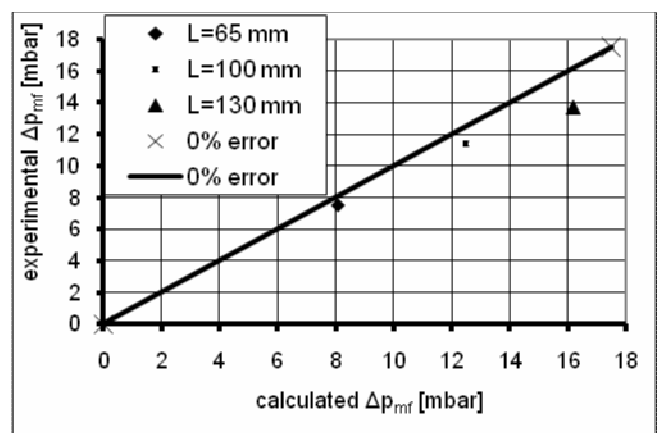


Fig. 9: The comparison of experimental and calculated Δp_{mf} for 210 μ m quartz sand

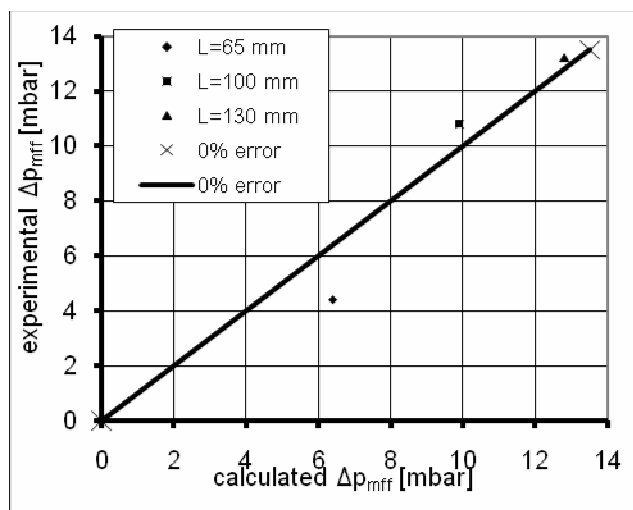


Fig. 10: Comparison of experimental and calculated Δp_{mff} for 210 μ m quartz sand

Table 3: Measurements results

Symbol	Value	[unit]
p_1	34.4	mbar
p_2	11.3	mbar
p_3	0.2	mbar
p_4	0.1	mbar
p_5	6.2	mbar
p_6	3.9	mbar
p_7	3.2	mbar
v_{gas}	5.1	m/s
v_{comb}	9	m/s

Relative pressures were measured at a stationary state. One of the experiments was made when testing the process with quartz sand where the average particle diameter was about 210 μ m. The stationary bed height in the reactor was 100 mm and the mass of sand used at simulation was 4.25 kg. When minimum fluidization conditions were obtained, the bed height increased by approximately 15mm. A series of repeated measurements was carried out and the average relative pressure at the bottom of the fluid bed was $p_2 = 11.3$ mbar, with $p_3 = 0.2$ mbar the average value at the top. As follows from this, the pressure drop across fluidized bed was $p_{2,3} = 11.1$ mbar. Air flow had an average temperature of 25 °C. Inlet gas velocity was about 5.1 m/s in the reactor and 9 m/s in the combustion zone. We found a higher gas velocity for fluidization than calculated, due to a certain amount of air passing through the chute to the combustion zone. This also provides the explanation as to why the measured terminal velocity in the combustion zone was a little lower than

anticipated, as the loss of air from the reactor helped increase the air speed in the combustion zone – resulting in the aforementioned lower value.

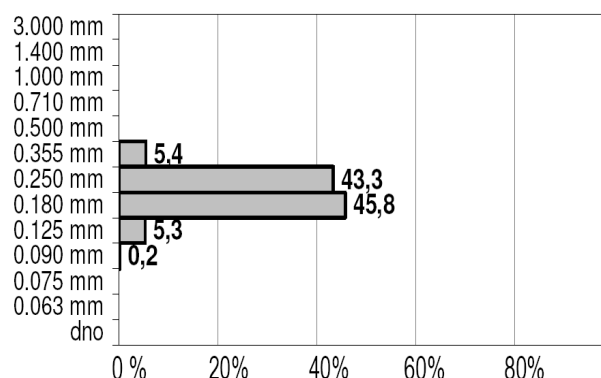


Fig. 11: The size of the particles used for simulation

7 Conclusions

By observing the FICFB processes in a three-times smaller laboratory unit with air flow the size and density of particles has been determined. The preferred option was to use brass powder with an average particle diameter of 200 μ m. The assumption of particle flow similarity is based on a direct comparison of Reynolds numbers. In this case the Re_p are 9.8 and 9.0 in reactor and 46.6 and 50.8 in the combustion zone. There is a 10% difference between Re_p in both cases. Chemical reactions cause variations in temperature, density, and dynamic viscosity all of which affect Re_p . If we compare Re_p 9.8 and 4.9 at the reactor exit 46.6 and 23.3 at the top of the combustion zone exit, we can see that Re_p changes by 50 % and the similarity at this point is actually questioned. By way of example, the experiment carried out with quartz sand was presented. When the process is stabilized and a smooth circulation is established, then pressure drops are as follows: $p_{2,3} = 11.2$ mbar, $p_{6,7} = 0.7$ mbar, $p_{2,6} = 7.4$ mbar and $p_{4,7} = -3.1$ mbar. This result set can be characterized as $p_2 > p_6$ and $p_4 < p_7$. Pressures are as expected and gas flows are in the appropriate directions. Through the application of the mathematical models we have, pressure drops can be predicted to within a 20% error margin. The experiments highlighted one major problem, namely that the cylindrical tube and asymmetric enlargement of the tube didn't prove to be a successful construction for the reactor. With beds higher than 13 cm fluidized beds are in aggregative or bubbling fluidization states. In turn, at bed heights over 30 cm even a slugging state is attained. The solution at this point is a conical bed design in accordance with Kaewklum and Kuprianov [16].

Symbols:

A_p	Cross-section of particle	[m ²]
A_t	Tube cross-section	[m ²]
C_x	Drag coefficient	
D_{com}	Combustion zone diameter	[mm]
$D_{gas,1}^b$	Diameter of reactor upper segment	[mm]
$D_{gas,2}^b$	Diameter of reactor lower segment	[mm]
D_p	Diameter of particle	[μm]
D_{tube}	Inside tube diameter	[mm]
$F_{g,p}$	Gravity of particle	[N]
g	Gravity acceleration	[9,81 m/s ²]
g_c	Conversion factor	[9,81 gm m/s ² wt]
H_{com}^b	Combustion zone height	[mm]
i	Natural number	
j	Natural number	
L	Stationary bed height	[m]
L_{mf}	Bed height at minimum fluidization condition	[m]
L_{mff}	Bed height at minimum fully fluidized state	[m]
p	Pressure	[Pa]
$p_{g,ar}$	Pressure at arbitrary conditions	[Pa]
p_i	Relative pressure in point i	[Pa]
$p_{i,j}$	Differential pressure between points i and j	[Pa]
p_j	Relative pressure in point j	[Pa]
p_n	Pressure at normal conditions	[Pa]
Re_p	Particle Reynolds number	
$T_{g,ar}$	Temperature at arbitrary conditions	[°C]
T_n	Temperature at normal conditions	[°C]
v_{comb}	Gas velocity in combustion zone	[m/s]
v_g	Gas velocity	[m/s]
v_{gas}	Gas velocity in gasification zone	[m/s]
v_{mf}	Minimal fluidization velocity	[m/s]
v_{mff}	Minimal velocity of full fluidization	[m/s]
v_t	Terminal velocity	[m/s]
Δp	differential pressure	[Pa]
Δp_{mf}	differential pressure at minimum fluidization	[Pa]
Δp_{mff}	differential pressure at full fluidization	[Pa]
ϵ_{mf}	Bed voidage at minimum fluidization	
ϵ_{mff}	Bed voidage at full fluidization	
η_g	Dynamical viscosity of gas	[Pa·s]
$\eta_{g,ar}$	Dynamical viscosity of gas at	[Pa·s]

arbitrary conditions

η_n	Dynamical viscosity of gas at normal conditions	[Pa·s]
Φ_m	Mass flow	[kg/h]
$\Phi_{m,g}$	Mass flow of gas	[kg/h]
Φ_V	Volume flow	[m ³ /h]
$\Phi_{V,g}$	Volume flow of gas	[m ³ /h]

References:

- [1] Daizo Kunii, Octave Levenspiel, *Fluidization Engineering*, John Wiley & Sons, inc., 1969
- [2] Leon R. Glicksman (1982), *Scaling Relationships For Fluidized Beds*, Chemical engineering science, 39, 1373-1384
- [3] M. T. Nicastro, Leon R. Glicksman (1982), *Experimental Verification of Scaling Relationships for Fluidized Beds*, Chemical engineering science, 39, 1373-1384
- [4] G. Löffler, S. Kaiser, K. Bosch, H. Hofbauer (2003), Hydrodynamics of a Dual Fluidized - Bed Gasifier - Part I : Simulation of a Riser With Gas Injection and Diffuser, *Chemical Engineering Science*, 58, 4197 – 4213
- [5] S. Kaiser, G. Löffler, K. Bosch, H. Hofbauer (2003), Hydrodynamics of a Dual Fluidized Bed Gasifier - Part Ii: Simulation of Solid Circulation Rate, Pressure Loop and Stability, *Chemical Engineering Science*, 58, 4215 – 4223
- [6] Perry, R. H. (1988), *Perry's Chemical Engineers Handbook (6th ed.)*, New York: McGraw Hill International Ed.
- [7] Janez Oman, *Generatorji Toplote*, University in Ljubljana, Faculty of mechanical engineering, Ljubljana, 2005
- [8] Harrie Knoef, *Handbook Biomass Gasification*, BTG Biomass technology group, The Netherlands, 2005
- [9] Janez Oman, A. Senegačnik, A. Mirandola, *Air, Fuels and Flue Gases: Physical Properties and Combustion Constants*, Edizioni Libreria Progeto, Padova, Italy, 2006
- [10] Bojan Kraut, *Strojniški priročnik*, Tehniška založba Slovenije, 2000
- [11] N.I.Koškin, M.G.Širkevič, *Priročnik elementarne fizike*, Tehniška založba Slovenije, 1990
- [12] Nicolas Abatzoglou, *Green Diesel for Fisher-Tropsch Synthesis: Challenges and Hurdles*, 3rd WSEAS/IASME International Conference on Energy, Environment, Ecosystems and Suitable development, July 2007, Greece
- [13] Franz Binder, Andreas Werner, *Investigations of solids inventory and particle size distribution in a pressurized circulating fluidised bed combustor*, Proceedings of the 4th WSEAS Int.

- Conf. on Heat Transfer, Thermal Engineering and Environment, Greece, August 21-23, 2006 (pp1127-132)
- [14] Mladen Stanojević, Sanja Vraneš, Iskender Gokalp, *Preliminary Remarks on Socio-Economic Impacts of Biofuel Production and Use in Europe*, Proceedings of the 2006 IASME/WSEAS International Conference on Energy & Environmental Systems, Greece, May 8-10, 2006 (pp260-265)
- [15] Miroslava Smitkova, František Janiček, *Evaluation of the Westinghouse cycles*, WSEAS Transactions on Power Systems, May 2008
- [16] Rachadaporn Kaewklum, Vladimir I. Kuprianov, *Theoretical And Experimental Study On Hydrodynamic Characteristic Of Fluidization In Air-Sand Conical Beds*, Chemical Engineering Science 63 (2008) 1471-1479